Structures, stabilities and electronic properties of C 50 dimers

ARTICLE *in* JOURNAL OF MOLECULAR STRUCTURE THEOCHEM · DECEMBER 2010

Impact Factor: 1.37 · DOI: 10.1016/j.theochem.2010.08.033

4 AUTHORS, INCLUDING:

Hongcun Bai
Ningxia University
32 PUBLICATIONS **113** CITATIONS

SEE PROFILE

Journal of Molecular Structure: THEOCHEM 961 (2010) 42–47

Contents lists available at ScienceDirect

Journal of Molecular Structure: THEOCHEM

journal homepage: www.elsevier.com/locate/theochem

Structures, stabilities and electronic properties of C_{50} dimers

Hongcun Bai, Ruiying Du, Weiye Qiao, Yuanhe Huang *

College of Chemistry, Beijing Normal University, Beijing 100875, China

ARTICLE INFO

Article history:
Received 6 June 2010
Received in revised form 27 August 2010
Accepted 31 August 2010
Available online 8 September 2010

Keywords:
C_{50}
Fullerene dimers
Stability
Electronic structures
Frequency analysis

ABSTRACT

The dumbbell-shaped dimers constructed from C_{50} cages are investigated using self-consistent field molecular orbital method based on density functional theory. Our study focuses on the structures, stabilities, electronic and vibrational properties of the C_{50} dumbbell-shaped dimers. It is found that the stability of these C_{50} dimers is related to bonding positions and linking patterns. For the dimers by [2 + 2] cycloaddition, a simple rule is proposed to predict the stabilities of these additive products of fullerenes according to the environment around the C–C bonds on the addition position. Moreover, higher thermodynamic stability is accompanied with larger HOMO–LUMO gaps for these dimers. The vibrational properties of the C_{50} dimers are also discussed in this paper.

1. Introduction

Fullerenes have aroused considerable attention since the discovery of C_{60} in 1985 [1]. Because carbon cages smaller than C_{60} violate the isolated pentagon rule (IPR) [2], small fullerenes with lower stabilities have been synthesized successfully only recent years. Zettl's group claimed the fullerene C_{36} was prepared [3], and later the smallest fullerene C_{20} was produced by Prinzbach and co-workers [4]. In 2004, Xie et al. [5] successfully synthesized the first C_{50} derivative, $C_{50}Cl_{10}$, which attracts interest in C_{50} and its derivatives [6–12].

Compared with C_{60}, small carbon cages have higher strain and reactivity due to the adjacent pentagons, thus they are good candidates to form dimers, oligomers and polymers [12–14]. Several possible structures of the dumbbell-shaped dimers constructed from C_{50} cages have been given in the previous studies [6,10,12]. The formal [2 + 2] dimer via the equatorial pentagon–pentagon junctions is the most stable dumbbell-shaped C_{50} dimer according to the results of Lu et al. [6]. However, only a few structures among the numerous possible C_{50} dimers are mentioned in the previous studies. Additionally, the smaller fullerene dimers are of prominent importance since they are the building blocks of various fullerene polymerized arrays. Thus, a more comprehensive study on the C_{50} dimers is still worth doing for the further understanding of structure–property relationship of the nanoscale structures built from C_{50} cages.

In this paper, we perform a theoretical study on the dumbbell-shaped C_{50} dimers built from D_{5h} C_{50} cages using self-consistent field molecular orbital (SCF-MO) method based on density functional theory (DFT). The studies focus on the structures, stabilities, electronic and vibrational properties of the dimers. The obtained results of C_{50} dimers are compared with those of the dimers composed of C_{60}, C_{36} and C_{20} cages.

2. Models and computational methods

We consider the dumbbell-shaped C_{50} dimers with higher symmetry. Here, D_{5h} C_{50} cages are used to construct these dimers, since D_{5h} C_{50} cage has highest symmetry among C_{50} isomers. It has been proved that the skeleton of synthesized $C_{50}Cl_{10}$ has D_{5h} structure [5]. Hartree–Fock calculations gave that D_{5h} C_{50} cage had the lowest energy [7,8], but DFT and MP2 results showed that a C_{50} isomer with D_3 symmetry was more stable than the D_{5h} cage [6,8,11]. The structure of D_{5h} C_{50} is shown in Fig. 1. In D_{5h} C_{50}, there are four non-equivalent carbon atoms which are labeled as C1, C2, C3 and C4 in Fig. 1, respectively. The bond lengths of D_{5h} C_{50} optimized at B3LYP/6-31G(d) level are also listed in Fig. 1. Our results agree quite well with the previous DFT and MP2 calculations [6,8].

The dumbbell-shaped C_{50} dimers are classified as three categories according to their joining patterns: the single-bonded (SB) dimers, the double-bonded (DB) dimers and the multiple-bonded (MB) dimers. The C_{50} dimers with possible higher symmetries are considered for DB and MB dimers. As for the SB dimers, two structures with C1 symmetry (SB-3 and SB-4) are also considered for the comparison. Thus, totally 32 different dumbbell-shaped C_{50} dimers are obtained with full geometric optimization, including seven SB dimers, fourteen DB dimers and eleven MB dimers. According to our best knowledge, most of these dimers are studied for the first time except SB-1, DB-1, DB-2 and DB-3.

* Corresponding author. Tel.: +86 010 58805425; fax: +86 010 58802075.
E-mail address: yuanhe@bnu.edu.cn (Y. Huang).

0166-1280/$ - see front matter © 2010 Elsevier B.V. All rights reserved.
doi:10.1016/j.theochem.2010.08.033

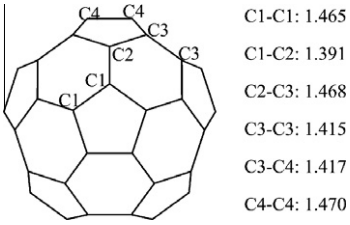

Fig. 1. Structure of D5h C_{50} (bond length in Å).

DFT-B3LYP hybrid functional method [15,16] is adopted to calculate the C_{50} dimers, because it has become an efficient tool for theoretical studies on fullerene nanostructures [6,7,9–12]. Both the geometrical optimizations and the electronic property calculations in this paper are all performed using SCF-MO method at 6-31G(d) level with Gaussian 03 program [17]. In the SCF-MO calculations, symmetry constraint is always adopted.

3. Results and discussion

3.1. Structures of the C_{50} dimers

The optimized structures and symmetries of the C_{50} dimers are shown in Fig. 2. From Fig. 2 we can see that the intercage bond lengths of the seven SB dimers rank from 1.561 Å to 1.625 Å. These bonds are longer than the traditional C–C single bonds (1.54 Å in diamond), but similar to those of the C_{60} SB dimers (1.663 Å in Ref. [18]). For the DB dimers, the intercage bond lengths are between 1.568 Å and 1.727 Å. It has been shown that the intercage bonds of C_{60} DB dimers (via 6/6 bond of C_{60}) are 1.576 Å by X-ray diffraction [19] and 1.575–1.594 Å by DFT calculations [10,20]. A systematic study on DB dimers of fullerenes C_n (n = 50–60) [10] suggested that the bond lengths ranged from 1.570 Å to 1.612 Å. Thus the C_{50} DB dimers have the similar intercage bond lengths with other fullerene DB dimers. DB-1, obtained by [2 + 2] cycloaddition via bond C4–C4 in C_{50}, presents the intercage bond length of 1.592 Å, which is closed to the results of 1.593 Å and 1.601 Å by DFT calculations [6,10]. As for the MB dimers, the intercage bond lengths of 1.509–1.709 Å have larger dispersion than those of the SB and DB dimers. However, these bond lengths can still be considered as in range of the C–C single bond length. Thus, it seems that the dimers composed of the carbon cages are inclined to connect through covalent bonds with the single bond length.

3.2. Stabilities of C_{50} dimers

In order to evaluate the thermodynamic stability of C_{50} dimers, the binding energy (E_b) of the C_{50} dimers is defined as:

$$E_b = E(\text{dimer}) - 2E(C_{50}) \quad (1)$$

where E(dimer) and $E(C_{50})$ are the energies of a C_{50} dimer and a D_{5h} C_{50} cage. The formation of the dimers is favorable to the stability of these systems when $E_b < 0$. The formation of a dimer is the result of interaction between the two carbon cages. Usually, the bonding interaction is a stable factor for the dimers. However, the formation of intercage bonds will also be concomitant with the deformation of C_{50} cages. If the deformation causes larger strain energy, it will reduce stability of the system. The deformation energy (E_d) of the two carbon cages and the interaction energy (E_i) between the two deformed cages are defined as follows:

$$E_d = E_{1d} + E_{2d} - 2E(C_{50}) \quad (2)$$

$$E_i = E(\text{dimer}) - E_{1d} - E_{2d} \quad (3)$$

where E_{1d} and E_{2d} are the energies respectively for each of the two deformed C_{50} cages. The calculated E_b, E_d and E_i for the C_{50} dimers are listed in Table 1.

From Table 1, it can be seen that the deformation effect for all the C_{50} dimers is endoergic, it is because the carbon cages distorted from their minimum energy structures for the formation of a dimers. This is similar to the case in silicon-doped C_{60} dimers [21]. Moreover, the dimers with the same linking pattern have very close values of E_d, about 2 eV and 5 eV for SB and MB dimers, respectively. As for the DB dimers, the E_d values are about 3 eV, except for DB-2, DB-3 and DB-12. The connections between two C_{50} cages are side-to-face or face-to-face in the three DB dimers, not side-to-side, resulting in larger structural deformation and lager E_d. Thus, the deformation energies are mainly determined by the connecting patterns, which would be one of the factors contributed to the stabilities of these dimers. As for the interaction effect, it is exothermic for all the dimers except for MB-10 and MB-11, indicating that the interaction between the two deformed carbon cages plays stable role in most of these C_{50} dimers. Moreover, E_i is quite different from the different dimers with the same linking pattern. From Eqs. (1)–(3), it is easy to get $E_b = E_i + E_d$. Hence, the change of binding energies should be mainly related to the change of the interaction energies for the dimers with the same linking pattern. From Table 1, we can see that the values of E_b follow exactly the same increasing or decreasing trend as those of E_i, which is also similar to the case in the silicon-doped C_{60} dimers [21]. Thus, we may conclude that the relative order of stability is mainly dependent on the interaction effect for the C_{50} dimers with the same linking pattern. In addition, it can be seen that the formation of dimers with pure C4–C4 intercage bonds are all energetically favorable. On the contrary, the intercage bonds are all C1–C1 bonds in the most unstable structures for the DB and MB C_{50} dimers. In fact, the SB dimer with C1–C1 connection is also calculated, but the optimization leads to separation of the two C_{50} cages, the SB dimer with C1–C1 intercage bond cannot be formed. The stability is different from different intercage bonding sites for the dimers with the same linking pattern. These indicate that the bonding position also plays an important role in stability of the formed dimers.

It is known that the π-orbital axis vector (POAV) angle, which is defined as the angle between the π-orbital and adjacent σ-orbital minus 90° [22], can reflect the strain of a carbon atom in a fullerene cage. A large POAV angle causes larger strain on the sp2 carbon atom and high reactivity [22], thus bonding through the atoms having larger POAV angle should be more favorable to releasing the strain. Accordingly, the order of stability is related to the POAV angle of the non-equivalent atoms for the dimers. For the D_{5h} C_{50}, the POAV angles are 10.7°, 12.5°, 12.8° and 15.5° for C1, C2, C3 and C4, respectively [6]. Therefore, the intercage bonding through C4 should be most favorable to release strain of the carbon cages, resulting in the energetically favorable structures. In contrast, the bonding at C1 is most unfavorable to stability of the dimers. This is why the dimers with pure C4–C4 intercage bonds are all energetically favorable, but those dimers with pure C1–C1 intercage bonds all have positive E_b as mentioned above. From Table 1, it can be found that the stability of the SB dimers agrees well with the POAV angles of the intercage bonding atoms. Furthermore, the order of POAV angles can even determine order of the binding energies for the SB dimers constructed from the carbon cages with different size since there is only one intercage bond. The calculated E_b of the C_{20} SB dimer with the lowest energy [13] is smaller than that of the SB-1 by 1.303 eV at the same computational level. It comes as no surprise because the C_{20} has larger POAV angle than C_{50}. Besides, the formation of C_{60} SB dimer is even not energetically favorable with the B3LYP calculation [20], since the C_{60} has smaller POAV angle than C_{50}.

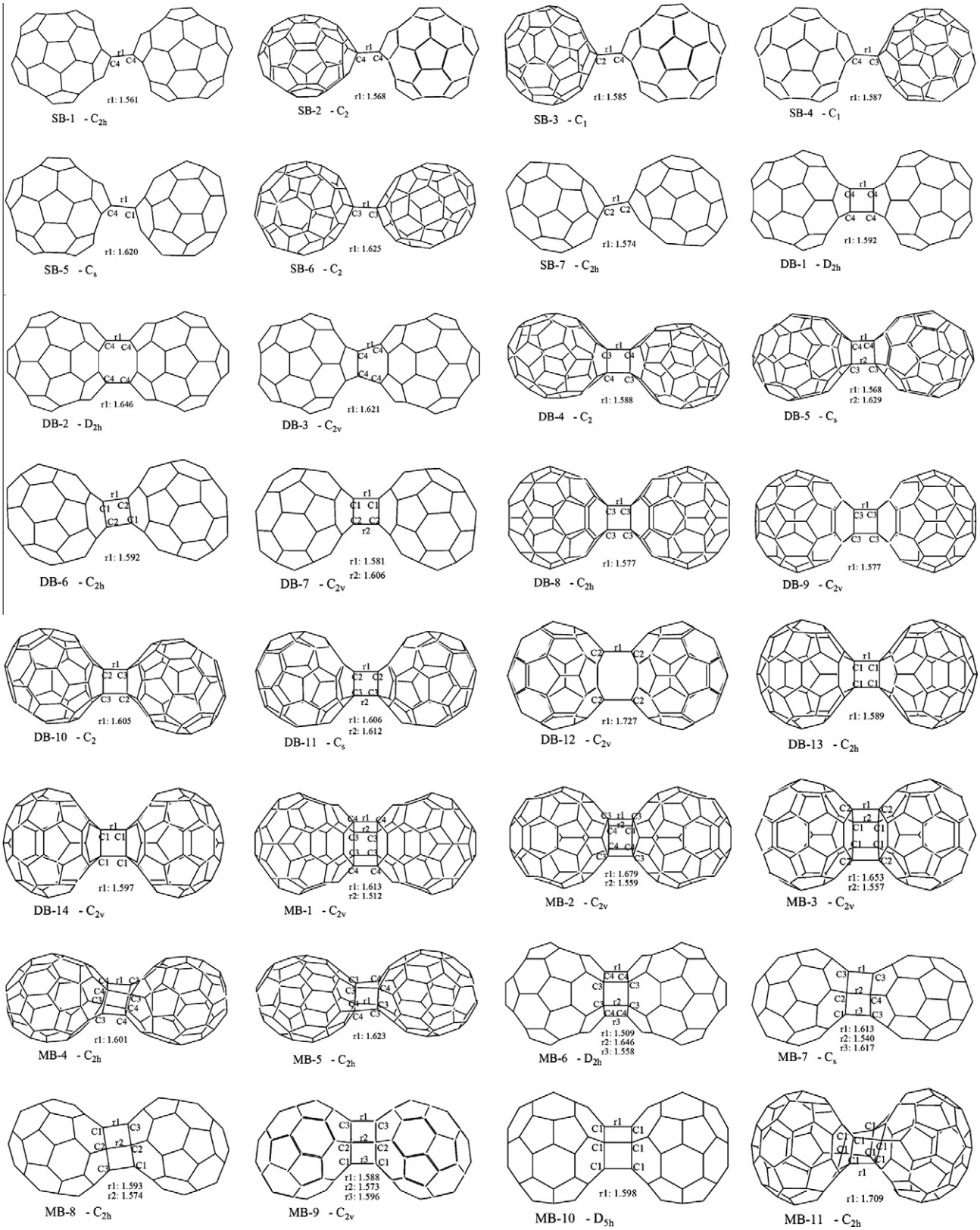

Fig. 2. Structures and symmetries of the C_{50} dimers (bond lengths in Å).

According to order of the POAV angles, the DB dimers with pure C4–C4 intercage bonds should be most stable, and those with pure C1–C1 intercage bonds are most unstable in view of energy, which agrees with our DFT calculations. Nevertheless, it can be seen that the DB dimers with C1–C2 bonds are more stable than those DB dimers with the C2–C2, C3–C3 and C2–C3 bonds, though the POAV angle of C1 is the smallest one. E_b of the formers is negative but those of the latter are positive. This shows that we cannot determine

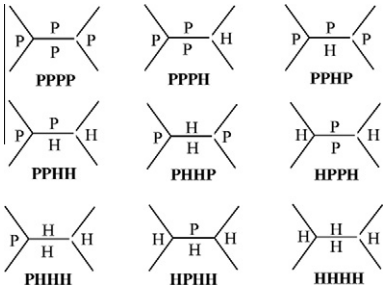

Fig. 3. Denotations for the C–C bonds in the fullerenes.

Table 1
Calculated energies and electronic properties of the C_{50} dimers (in eV).

Dimer	E_b	E_i	E_d	HOMO	LUMO	E_g
SB-1	−0.883	−2.743	1.860	−5.13	−4.59	0.55
SB-2	−0.849	−2.376	1.527	−5.13	−4.58	0.56
SB-3	0.054	−2.074	2.128	−5.17	−4.63	0.53
SB-4	0.113	−1.868	1.982	−5.06	−4.60	0.46
SB-5	0.382	−1.240	1.622	−5.17	−4.57	0.60
SB-6	1.017	−0.906	1.923	−5.02	−4.60	0.43
SB-7	1.021	−0.903	1.924	−5.16	−4.80	0.37
DB-1	−1.732	−4.263	2.531	−5.63	−3.81	1.82
DB-2	−1.166	−5.222	4.055	−5.80	−3.76	2.03
DB-3	−0.738	−5.379	4.641	−5.65	−3.80	1.84
DB-4	−0.728	−3.246	2.517	−5.65	−3.99	1.66
DB-5	−0.661	−3.264	2.603	−5.64	−4.00	1.64
DB-6	−0.255	−3.218	2.963	−5.50	−4.05	1.45
DB-7	−0.254	−3.222	2.968	−5.47	−4.08	1.39
DB-8	0.834	−2.026	2.860	−5.29	−4.22	1.07
DB-9	0.838	−2.027	2.864	−5.26	−4.21	1.05
DB-10	1.410	−2.030	3.440	−5.39	−4.18	1.21
DB-11	1.415	−1.922	3.338	−5.40	−4.18	1.19
DB-12	2.047	−2.786	4.833	−5.47	−3.78	1.69
DB-13	2.651	−0.775	3.426	−5.42	−4.41	1.01
DB-14	2.665	−0.720	3.385	−5.44	−4.37	1.07
MB-1	−1.055	−5.262	4.207	−5.72	−3.81	1.92
MB-2	1.160	−3.577	4.737	−5.60	−4.08	1.52
MB-3	1.178	−3.933	5.111	−5.44	−3.91	1.54
MB-4	1.575	−4.973	6.548	−5.63	−3.97	1.65
MB-5	1.999	−4.736	6.736	−5.65	−3.93	1.72
MB-6	2.517	−2.578	5.096	−5.61	−3.89	1.71
MB-7	2.964	−2.514	5.478	−5.30	−4.10	1.21
MB-8	3.396	−2.322	5.718	−5.26	−4.12	1.14
MB-9	3.458	−2.268	5.726	−5.23	−4.10	1.13
MB-10	6.367	1.024	5.343	−5.42	−4.69	0.73
MB-11	6.482	1.007	5.474	−5.46	−4.46	0.99
C_{50}				−5.54	−4.17	1.37

the stability order of the DB dimers just simply according to the order of the POAV angles. In these dimers, intercage bonding is through closed [2 + 2] cycloaddition, i.e., the side-to-side junction. Here, a side is a C–C bond. Therefore, the environment around the C–C bonds would affect strain release and reactive activity of the C–C bonds. It has been given that a vertex in a fullerene cage can be denoted by a set of three rings fused at this site [23,24], such as PPP, PPH, PHH and HHH, H denotes hexagon and P pentagon. Likewise, we use similar denotation to express a C–C bond as shown in Fig. 3. More pentagons around a C–C bond, especially the bond is a side of the pentagons, would introduce more strain and higher reactivity. Thus, a rule of the stability order for the bond to bond closed [2 + 2] cycloaddition of fullerenes is here suggested as follows: PPPP > PPPH > PPHP > HPPH > PPHH > PHHP > HPHH > PHHH > HHHH.

Among the C–C bonds in the C_{50} cage, C1–C1 and C2–C3 belong to HPHH, C1–C2 and C3–C3 PHHP, C3–C4 PPHH and C4–C4 HPPH. For the bonds with the same denotations but composed of different non-equivalent carbon atoms, the order follows the order of POAV angels of the atom sites. Hence, the stability order would be C4–C4 > C3–C4 > C1–C2 > C3–C3 > C2–C3 > C1–C1 for the dimers with the closed [2 + 2] structure, which agrees well with the results of our calculations. It is also found that the stability order of the C_{36} closed [2 + 2] DB dimers [25] also satisfies the rule suggested here. For the C_{70} cage, the types of C–C bonds are PHHP, HPHH, PHHH and HHHH, respectively. The addition of benzyne to C_{70} showed that the ratio of isomeric monoadducts on PHHP bonds is as high as 77%, the others are 13% and 10% respectively for HPHH and PHHH [26]. These ratios indicate that the stability and reactive order of the addition should be PHHP > HPHH > PHHH > HHHH, which is in accordance with our suggested rule. Moreover, 6/6 bond and 5/6 bond in C_{60} belong to PHHP and HPHH, respectively, so the [2 + 2] addition reactions occur to 6/6 bond not 5/6 bond [19]. Thus, the suggested rule may be useful to predict the stability order of adducts for the addition at both ends of a C–C bond of fullerene cages.

As to the MB dimers, most MB dimers are energetically unfavorable, and only formation of MB-1 is exothermic. Because of complicated intercage bonding, it is difficult to give POAV analysis for the stability of the MB dimmers. The distortion of the carbon cages is great for the MB dimers, and results in large deformation. This leads to lower stabilities for the MB dimers.

The dianion C_{50} dimers of SB-1, DB-1 and MB-1 are also calculated with full geometrical optimizations. Because of more electrostatic repulsions between the two carbon cages, the intercage bonds are increased more or less in the charged dimers compared to those of the neutral dimers. The relative energies of the dianion C_{50} dimers for SB-1, DB-1 and MB-1 are 0, 0.701, and 1.359 eV, respectively. Thus the order of stability for the charged dimers is: SB-1 > DB-1 > MB-1, which is different from that for the corresponding neutral dimers. The dianion C_{50} SB dimer is more stable than the DB and MB dimers, which is similar to the case in the dianion C_{60} dimers [20]. This manifests that the effects of extra charge on the stability are quite different from the dimers with different structures.

3.3. Electronic properties of C_{50} dimers

It is well-known that the frontier orbitals, the highest occupied molecular orbital (HOMO) and the lowest unoccupied molecular orbital (LUMO), play an important role in chemical reaction for the reactant molecule, thus the frontier orbital analysis of C_{50} dimers is necessary. In Table 1 we summarize the HOMO and LUMO energy levels of the C_{50} dimers. Although the Koopmans' theorem is not valid for DFT calculation, the relative positions of the HOMO and LUMO still reflect the abilities to lose and gain electrons. However, the ability to lose and gain electrons should no significant change compared with those of the C_{50} cage for the formations of the C_{50} dimers, since the energy levels of the frontier orbitals all vary small.

It is known that both the thermodynamic stability and kinetic stability have crucial influence on the relative abundances of different fullerene structures. It has been pointed out that kinetic stability is related with the HOMO–LUMO energy gap (E_g) [27], but the unweighted HOMO–LUMO gap alone as an index of kinetic stability of fullerene structures may not be valid [28]. Usually low chemical reactivity is associated with a large E_g, because exciting electrons from a low HOMO to a high LUMO is energetically unfavorable, which would be necessary to activate a reaction [27]. The calculated E_g of C_{50} dimers are listed in Table 1. It can be found that all the SB dimers present small E_g (about 0.5 eV). Energy gaps of the DB dimers are in the range of 1.01–2.03 eV, which are comparable with E_g of C_{50} (1.37 eV). For MB dimers, E_g disperse more widely, from 0.73 eV to 1.92 eV. It is noteworthy that the thermodynamic stability has something to do with the energy gaps for these

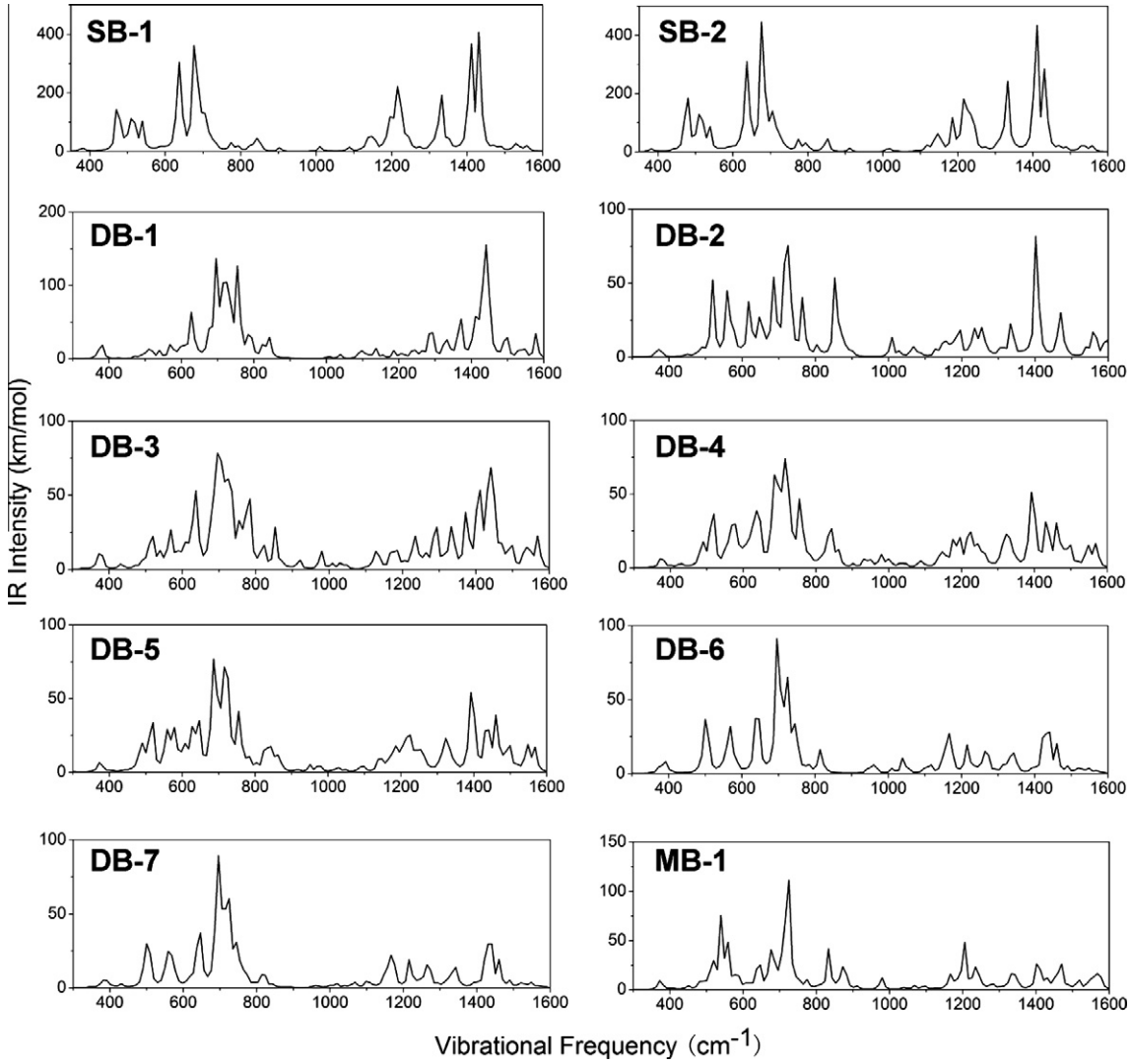

Fig. 4. Calculated IR spectra of the C_{50} dimers.

dimers. The energetically favorable dimers are mostly to have larger energy gaps compared to those energetically unfavorable dimers with the same pattern. The most stable three dimers DB-1, DB-2 and MB-1 also have the largest energy gaps. Thus, it appears that higher thermodynamic stability is possibly accompanied with higher kinetic stability for these dumbbell-shaped dimers in a view of the energy gap.

3.4. Vibrational analysis and infrared spectra

The formation of the dimers with minus binding energies is favorable to the stability of the systems from the point of view of energy. Here vibrational frequency analysis is performed at B3LYP/6-31G(d) level to verify whether these C_{50} dimers are local minima on the potential energy surface. The calculated vibrational frequencies for these dimers show no imaginary vibrational frequency, indicating that the structures of these C_{50} dimers correspond to the true minima on the potential energy surface. The irreducible representations of all vibrations of these dimers are listed as follows:

$$\Gamma_{SB-1-vib} = 69A_u(IR) + 78B_u(IR) + 79A_g + 68B_g$$

$$\Gamma_{SB-2-vib} = 148A(IR) + 146B(IR)$$

$$\Gamma_{DB-1-vib} = 35B_{1u}(IR) + 34A_u + 38B_{2u}(IR) + 41A_g + 38B_{1g} + 35B_{2g} + 40B_{3u}(IR) + 33B_{3g}$$

$$\Gamma_{DB-2-vib} = 34A_u + 35B_{1u}(IR) + 38B_{2u}(IR) + 40B3u(IR) + 41A_g(IR) + 38B_{1g} + 35B_{2g} + 33B_{3g}$$

$$\Gamma_{DB-3-vib} = 76B_2(IR) + 70B_1(IR) + 81A_1(IR) + 67A_2$$

$$\Gamma_{DB-4-vib} = 148A(IR) + 146B(IR)$$

$$\Gamma_{DB-5-vib} = 147A''(IR) + 147A'(IR)$$

$$\Gamma_{DB-6-vib} = 72A_u(IR) + 75B_u(IR) + 76A_g + 71B_g$$

$$\Gamma_{DB-7-vib} = 76A_1(IR) + 72A_2 + 75B_2(IR) + 71B_1(IR)$$

$$\Gamma_{MB-1-vib} = 76A_1(IR) + 72A_2 + 71B_1(IR) + 75B_2(IR)$$

where the vibrational modes of IR allowed by symmetry are labeled with *IR* in the brackets. As a matter of fact, many calculated IR intensities are very weak.

The calculated IR spectra of the dimers are presented in Fig. 4, which have been scaled by a factor of 0.98, according to the DFT study on the IR spectra of fullerene structures [29]. The strong

absorptions near 700 cm^{-1} are mainly derived from the vibrations of C2 and C3 atoms. The moderate peaks obtained near 1200 cm^{-1} and strong absorptions near the region of 1400 cm^{-1} are responsible respectively for the stretching vibration of C4–C4 bonds and C1–C2 bonds within the C_{50} cages. There are also some vibrations arising from the intercage bonding regions, which appear in the zone of 800–1000 cm^{-1}. It can be seen that the shapes of IR absorption spectra are different for the dimers with different structures. These characteristic features in the IR spectra could be helpful to identify these C_{50} dimers from the experimental spectra.

4. Conclusions

Based on DFT calculations, we have obtained the structures, stabilities and electronic properties of various possible C_{50} dimers. It is found that the C_{50} dimers DB-1, obtained by side-to-side connection via bond C4-C4 of D_{5h} C_{50}, is the most stable one among all the C_{50} dimers presented in a view of energy. The stability of C_{50} dimers is related to the bonding positions and the linking patterns as well as the distortion of the cages. We also find that the stability of the [2 + 2] side-to-side DB dimers is related with the environment around the C–C bonds on the addition sites and a simple rule is proposed as follows: PPPP > PPPH > PPHP > HPPH > PPHH > PHHP > HPHH > PHHH > HHHH. The higher thermodynamic stability is accompanied with larger HOMO–LUMO gaps for these dumbbell-shaped dimers. The calculated vibrational frequencies show different characteristic features for the C_{50} dimers with different structures.

Acknowledgement

This work is supported by the National Natural Science Foundation of China (Grant No. 20873009).

References

[1] H.W. Kroto, J.R. Heath, S.C. O'Brien, R.F. Curl, R.E. Smalley, Nature 318 (1985) 162.
[2] H.W. Kroto, Nature 329 (1987) 529.
[3] C. Piskoti, J. Yarger, A. Zettl, Nature 393 (1998) 771.
[4] H. Prinzbach, A. Weiler, P. Landenberger, F. Wahl, J. Worth, L.T. Scott, M. Gelmont, D. Olevano, B. Issendorff, Nature 407 (2000) 60.
[5] S. Xie, F. Gao, X. Lu, R. Huang, C. Wang, X. Zhang, M. Liu, S. Deng, L. Zheng, Science 304 (2004) 699.
[6] X. Lu, Z. Chen, W. Thiel, P.R. Schleyer, R. Huang, L. Zheng, J. Am. Chem. Soc. 126 (2004) 14871.
[7] X. Zhao, J. Phys. Chem. B 109 (2005) 5267.
[8] D. Wang, H. Shen, H. Gu, Y. Zhai, J. Mol. Struct.: THEOCHEM 776 (2006) 47.
[9] Z. Xu, J. Han, Z. Zhu, W. Zhang, J. Phys. Chem. A 111 (2007) 656.
[10] A. Bihlmeier, C.C.M. Samson, W. Klopper, ChemPhysChem 6 (2005) 2625.
[11] S. Diaz-Tendero, M. Alcami, F. Martin, Chem. Phys. Lett. 407 (2005) 153.
[12] L. Zhechkov, T. Heine, G. Seifert, J. Phys. Chem. A 108 (2004) 11733.
[13] Z. Chen, T. Heine, H. Jiao, A. Hirsch, W. Thiel, P.R. Schleyer, Chem. Eur. J. 10 (2004) 963.
[14] P.W. Fowler, D. Mitchell, F. Zerbetto, J. Am. Chem. Soc. 121 (1999) 3218.
[15] A.D. Beck, J. Chem. Phys. 98 (1993) 5648.
[16] C. Lee, W. Yang, R.G. Parr, Phys. Rev. B 37 (1988) 785.
[17] M.J. Frisch, G.W. Trucks, H.B. Schlegel, G.E. Scuseria, et. al., Gaussian 03 (Revision C.02), Gaussian, Inc., Wallingford CT, 2004.
[18] J. Kurti, K. Nemeth, Chem. Phys. Lett. 256 (1996) 119.
[19] G.W. Wang, K. Komatsu, Y. Murata, M. Shiro, Nature 387 (1997) 583.
[20] G.E. Scuseria, Chem. Phys. Lett. 257 (1996) 583.
[21] P. Marcos, J. Alonso, M. Lopez, J. Chem. Phys. 126 (2007) 44705.
[22] R.C. Haddon, Science 261 (1993) 1545.
[23] M. Lin, Y. Chiu, J. Xiao, J. Mol. Struct.: THEOCHEM 489 (1999) 109.
[24] P.W. Fowler, T. Heine, J. Chem. Soc., Perkin Trans. 2 (2001) 487.
[25] Y.M. Chen, Y.X. Li, Y.H. Huang, R.Z. Liu, Acta Chim. Sinica 58 (2000) 1511.
[26] M.S. Meier, G.W. Wang, R.C. Haddon, C. Brock, M. Lloyd, J.P. Selegue, J. Am. Chem. Soc. 120 (1998) 2337.
[27] H. Kietzmann, R. Rochow, G. Gantefr, W. Eberhardt, K. Vietze, G. Seifert, P.W. Fowler, Phys. Rev. Lett. 81 (1998) 5378.
[28] J. Aihara, Theor. Chem. Acc. 102 (1999) 134.
[29] R.E. Stratmann, G.E. Scuseria1, M.J. Frisch, J. Raman Spectrosc. 29 (1998) 483.